J Fluoresc (2013) 23:137–146
DOI 10.1007/s10895-012-1127-0

ORIGINAL PAPER

Highly Sensitive Optical Biosensor for Thrombin Based on Structure Switching Aptamer-Luminescent Silica Nanoparticles

Ethiraju Babu · Paulpandian Muthu Mareeswaran · Seenivasan Rajagopal

Received: 26 May 2012 / Accepted: 2 September 2012 / Published online: 11 September 2012

Abstract We describe here the construction of a sensitive and selective optical sensor system for the detection of human α-thrombin. The surface functionalized luminescent $[Ru(dpsphen)_3]^{4-}$ (dpsphen-4,7-diphenyl-1,10-phenanthroline disulfonate) ion doped silica nanoparticles (SiNPs) with a size ~70 nm have been prepared. The DABCYL (2-(4-dimethylaminophenyl)diazenyl-benzoic acid) quencher labeled thrombin binding aptamer is conjugated to the surface of SiNPs using BS^3 (bis(sulfosuccinimidyl) suberate) as a cross-linker, resulting in the conformational change of aptamer to form G-quadruplex structure upon the addition of thrombin. The binding event is translated into a change in the luminescence intensity of Ru(II) complex via FRET mechanism, due to the close proximity of DABCYL quencher with SiNPs. The selective detection of thrombin using the SiNPs-aptamer system up to 4 nM is confirmed by comparing its sensitivity towards other proteins. This work demonstrates the application of simple aptamer-SiNPs conjugate as a highly sensitive system for the detection of thrombin and also it is highly sensitive towards thrombin in the presence of other proteins and complex medium such as BSA.

Keywords Aptamer · Ruthenium complex · Silica nanoparticle · Thrombin · Luminescence · Sensor

Electronic supplementary material The online version of this article (doi:10.1007/s10895-012-1127-0) contains supplementary material, which is available to authorized users.

E. Babu · P. M. Mareeswaran · S. Rajagopal (✉)
School of Chemistry, Madurai Kamaraj University, Madurai 625 021, India
e-mail: rajagopalseenivasan@yahoo.com

Introduction

Aptamers, artificial single-stranded DNA or RNA oligonucleotides, are obtained through in vitro selection method called systematic evolution of ligands by exponential enrichment (SELEX) from the random RNA or DNA libraries [1, 2]. The aptamers bind specifically with a wide range of chemical or biological entities like small molecules, metal ions, peptides, nucleotides, proteins, and whole cell [3–10]. Since their first discovery in the 1990s, aptamers have attracted intense research efforts and in recent years started to find potential applications as biosensor, in drug delivery and in therapeutics [11–15]. A variety of aptamer based biosensors have been developed in the last few years pioneering electrochemical, fluorescence, chemiluminescence, surface plasmon resonance, AFM and microgravimetric techniques [16–21]. The luminescence technique is the simple and most sensitive method and finds wide range of applications [22].

The rapidly evolving nanotechnology has been used to design a variety of novel approaches based on nanoparticles for biological applications [23, 24]. Recent reports highlight the development of dye doped silica nanoparticles (SiNPs) based biosensor as one of the most efficient methods for tumor diagnosis, imaging and drug delivery [25, 26]. Luminescent SiNPs possess some key advantages over the conventional organic dyes such as high optical intensity, nontoxicity, more stability against photobleaching, easy modification and biocompatibility with biological systems [27, 28]. Moreover, the surface of SiNPs provides a robust stable shell and facilitates functionalization, either through physical adsorption or covalent attachment [29, 30]. The modification of SiNPs surface with carboxylic acid, cyanuric chloride, aldehyde, and NHS (N-hydroxysuccinimide) esters favors the grafting of bioreceptors for the detection

of target analytes [31–33]. Meanwhile, the high density of silica (1.96 g/cm^3) facilitates easy separation of NPs (Nanoparticles) from the mixture of various molecules via centrifugation, which could retain the target binding ability to promote trace detection of target in a mixture and in biological samples. Chen et al. [10] reported that the aptamer conjugated luminescent SiNPs can be used for the simultaneous diagnosis of multiple cancer cells.

Tan et al. have demonstrated the use of dye doped SiNPs for optical tagging with various biomedically important targets such as nucleic acid, cancer cells, bacterial cells and individual biomolecules [34–37]. The $[Ru(bpy)_3]^{2+}$ ion (bpy–2,2′-bipyridine) doped SiNPs-aptamer conjugate was used to amplify the signal intensity of the probe compared to individual Ru-bpy labeled aptamer and to minimize the photobleaching effect [38]. Recently, Liu et al. reported the label-free naked-eye detection of lysozyme using aptamer-functionalized SiNPs as the recognition element to capture the target and an anionic conjugated polymer as luminescent probe via electrostatic interaction [39].

Thrombin is a serine protease that regulates the process fibrinogen to fibrin and platelet activation to help stop bleeding [40]. The concentration of thrombin plays multiple pivotal role in thrombosis, hemostasis, blood coagulation, heart disease, central nervous system injury and Alzheimer's disease [41–43]. Thrombin is a major target for anticoagulation and cardiovascular disease therapy. When the concentration of thrombin is low (50 pM to 100 nM) it is responsible for neuroprotection hostility to ischemia, anti-inflammatory, oxidative stress, hypoglycemia, hypoxia and unexpectedly finds a barrier protective activity. If the concentration of thrombin is high, it will cause the degeneration and cell death in brain, spinal cord glial cell and the abnormal development of hippocampal will affect the memory leading to Alzheimer's disease [44, 45]. The design of thrombin sensor with extreme sensitivity and excellent selectivity is important for medical diagnostics.

Here we select thrombin as a model protein and its 15-mer thrombin binding aptamer as the receptor [46, 47]. We report a new strategy for the detection of thrombin using the luminescent SiNPs-aptamer conjugate system as the biosensor. The sensor system is constructed through $[Ru(dpsphen)_3]^{4-}$ (dpsphen-4,7-diphenyl-phenanthroline disulfonate) ion doped SiNPs labeled with aptamer at the one end and the DABCYL quencher in the other terminal.

Materials and Methods

Reagents

$RuCl_3.nH_2O$, disodium(4,7-diphenyl-1,10-phenanthroline disulfonate).$3H_2O$ (dpsphen), Triton X-100, tetraethyl orthosilicate (TEOS), aminopropyltriethoxysilane (APTES), (bis(sulfosuccinimidyl) suberate (BS^3), thrombin, BSA (bovine serum albumin), lysozyme, myoglobin, cytrochrome C and PDGF (platelet derived growth factor) were purchased from Sigma Aldrich and used as such without further purification. Sodium chloride, potassium chloride, disodium phosphate, sodium phosphate, ammonia solution and all the solvents purchased from Merck were used as such. The $[Ru(dpsphen)_3]^{4-}$ complex was prepared using the previous literature method [48]. The amino functionalized oligonuceotide, NH_2-$(CH_2)_6$-GGTTGGTGTGGTTGG-$(CH_2)_6$-DABCYL, was purchased from Ocimum Biosolutions Ltd. (Hyderabad, India). All the samples prepared using 1X PBS buffer pH 7.4 (8 g NaCl, 0.2 g KCl, 1.44 g Na_2HPO_4, 0.24 g KH_2PO_4 in 800 mL of Milli Q water) were used.

Instruments

The prepared surface modified luminescent SiNPs were characterized by HR-TEM, SEM and EDX measurements. The aptamer concentration was verified spectrophotometrically monitoring the absorbance at 260 nm, on Analtikjena Specord S100 diode-array spectrophotometer. The emission intensity was measured in the absence and presence of proteins with 100 μl of modified aptamer. The emission spectra were recorded using JASCO FP6300 Spectrofluorimeter in ambient temperature (298 K) and the 1 cm path length cuvette. All the fluorescence quenching measurements were carried under aerated condition. The AFM image was obtained on a PicoPlus AFM instrument (Molecular Imaging Inc., Arizona, USA) operating in the non-contact mode. AFM images were taken under dry condition. The NCL cantilever was used to scan the sample at a frequency of 177 KHz, and with a scanning speed 2.4 lines/s. The scanning electron microscopy (SEM) and energy dispersive X-Ray (EDX) micrographs were obtained by using a Hitachi S-3400 N model (Acc.Voltage 0.3 to 20 kV) and 2500 magnitude. The TEM image was taken from Sapera H7650 at 100 kV. Circular dichroism (CD) measurements were performed on a JASCO J810 spectropolarimeter at RT over the wavelength 200–300 nm. Parameters were set as follows: path length, 50 mm; resolution, 0.5 nm; scan speed, 50 nmmin^{-1}; band width, 1 nm; response 1 s. The CD measurements were made by keeping the concentration of aptamer (50×10^{-12}M) as constant while varying the concentration of thrombin (20×10^{-9} and 50×10^{-9}M).

Preparation of Surface-Modified $[Ru(dpsphen)_3]^{4-}$-doped SiNPs

The amine functionalized $[Rudpsphen_3]^{4-}$ ion doped SiNPs were synthesized according to previously published

procedure [49]. Briefly, the water-in-oil microemulsion was prepared from the solutions of 1.77 mL of Triton X-100, 7.5 mL of cyclohexane, 1.8 mL of *n*-hexanol, 400 μL of water, and 50 μL of 0.05 M $[Rudpsphen_3]^{4-}$ complex. This solution was stirred for 1 h, and then 200 μL of TEOS added as a precursor for silica nanoparticle formation, followed by the addition of 100 μL of NH_4OH to initiate the polymerization process. The reaction was allowed to continue for 24 h at room temperature to form $[Rudpsphen_3]^{4-}$ ion doped SiNPs with free hydroxyl groups. The amine terminated SiNPs were prepared from additional coating with addition of 100 μL of APTES followed by 50 μL of TEOS in the water-in-oil microemulsion containing hydroxy-SiNPs (OH-SiNPs) through the synchronous hydrolysis [49]. Afterwards the dye doped SiNPs were obtained by centrifugation and washed with ethanol, water and acetonitrile. Then the SiNPs were suspended in PBS buffer with ultrasonication for further experiments.

Covalent Immobilization of Aptamer onto the SiNPs Surface

Following the previously reported procedure [50], the aptamer conjugated with $[Rudpsphen_3]^{4-}$ ion doped SiNPs were prepared. A 50 μL of amine functionalized $[Ru(dpsphen)_3]^{4-}$ ion doped silica nanoparticles in PBS buffer at pH 7.4 was added to 30 μL of BS^3 (1 mg/mL). After 30 min incubation the solution was centrifuged for 3 mins (RCF of 1000×g) and then the supernatant was removed. A sample of 40 μL of the amine terminated DABCYL labeled aptamer (0.4 nM) was added to the SiNPs-BS^3 complex and shaken for 2 h. Finally we fabricated the sensor system $[Ru(dpsphen)_3]^{4-}$ ion doped SiNPs-aptamer conjugate by centrifugation and redispersed in PBS buffer using ultrasonication for other experiments, and the synthetic details are shown in Figure S1 in supporting information.

Results and Discussion

Principle of the Design of Luminescent Biosensor

The schematic illustration of thrombin detection based on the aptamer conjugated $[Ru(dpsphen)_3]^{4-}$ ion doped SiNPs is shown in Fig. 1. This sensor platform contains DABCYL quencher at 3′ of the DNA aptamer and the other end was immobilized with Ru-SiNPs via BS^3 coupling reagent. The formation of G-quadruplex is responsible for the close proximity of Ru-SiNPs and quencher resulting in the luminescence quenching in the presence of thrombin through fluorescence resonance energy transfer (FRET) [51]. The absorption and emission spectra of luminescent SiNPs are shown in Fig. S2.

Characterization of Ru(II) Complex Doped SiNPs

The $[Ru(bpy)_3]^{2+}$ and $[Ru(phen)_3]^{2+}$ ions doped SiNPs are well known and used as biosensor [38, 49, 52, 53]. Now, we have tried the derivatives of phen such as $[Ru(dpsphen)_3]^{4-}$ ion doped SiNPs prepared by modified Stober method and characterized by SEM, EDX (Figs. S3–S5, in supporting information) and TEM analysis. The advantage with the complex having dpsphen ligand is low toxicity than the bpy containing complex. The $[Ru(dpsphen)_3]^{4-}$ shows good water solubility because the ligand has both hydrophilic and hydrophobic moieties, hence it is used extensively in biological system [54]. After the SiNPs (~50 nm) were centrifuged the supernatant was taken for spectral measurements. The supernatant shows very weak absorption and emission intensity, indicating that almost all the dye molecules are incorporated into the SiNPs. Figure 2 shows the characteristic images of the surface modified luminescent SiNPs obtained after dispersion of sample on TEM grid and evaporation of solvent. From the SiNPs size and the density of silica (1.96 g/cm^3), it can be calculated that 1.0 mg of the synthesized SiNPs contained 1×10^{16} NPs. The SiNPs surface was modified with APTES to generate amino groups on the NPs surface for reaction with 30 μL of BS^3 in PBS buffer pH 7.4. This reaction yielded BS^3 conjugated SiNPs for aptamer immobilization. Finally 40 μL of amine functionalized aptamer was treated with SiNPs-BS^3 conjugate and obtained the SiNPs-aptamer system as the sensor platform for thrombin. The total number of immobilized aptamer (~120) molecules was calculated from the absorbance difference between the aptamer solution before and after incubation of the solution with SiNPs [39, 55].

Thrombin Assay

Upon addition of thrombin to SiNPs-aptamer conjugates the formation of intramolecular G-quadruplex [56] brings the quencher in the close proximity to the surface of SiNPs and this leads to a decrease in the luminescence intensity of Ru (II) complex, i.e., luminescence quenching (Fig. 3). This rearrangement favors the FRET from the luminescent $[Ru(dpsphen)_3]^{4-}$ ion doped SiNPs to nonluminescent DABCYL. In the absence of target molecule the aptamer prefers to form unfolded coil conformer. Thus the emission intensity of Ru(II) ion doped SiNPs are high in the absence of thrombin because the luminophore ($[Ru(dpsphen)_3]^{4-}$ ion) and quencher (DABCYL) are far away from each other. The decrease in the luminescence intensity in the presence of different concentrations of thrombin is associated with the amount of thrombin bound to the surface of aptamer conjugated SiNPs and Fig. 4 shows the emission intensity change with the addition of thrombin.

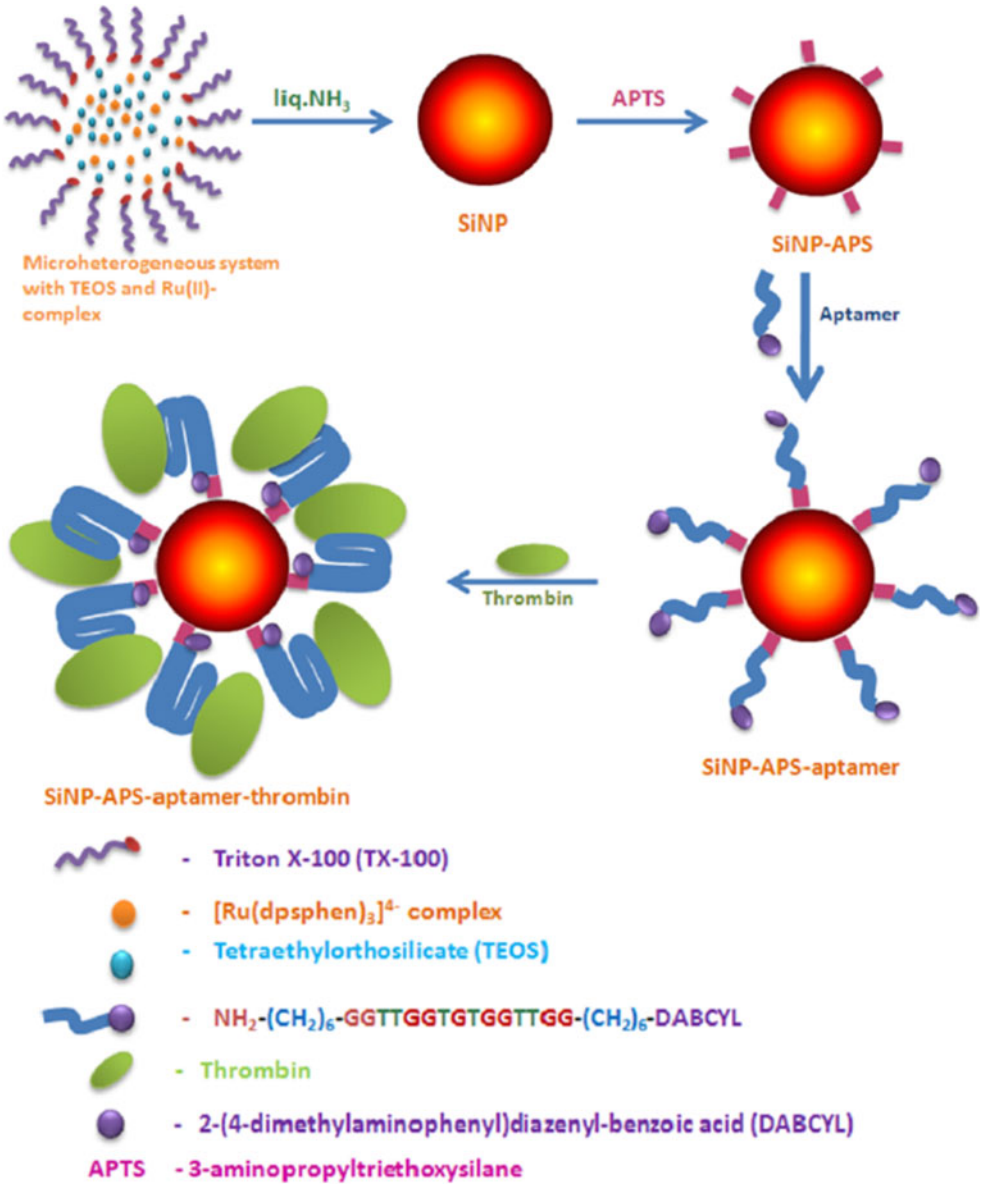

Fig. 1 Shematic representation of the detection system for thrombin using [Ru $(dpsphen)_3]^{4-}$ ion doped SiNPs-aptamer conjugate

The Stern-Volmer plot demonstrates the extent of luminescence quenching in the presence of thrombin and the equation shown in Eq (1) is used to get the Stern-Volmer [57] quenching constant.

$$I/I_0 = 1 + K_{SV}[Q] \quad (1)$$

$$K_{sv} = k_q \tau^{\circ} \quad (2)$$

where I_0 and I are the luminescence intensity in the absence and presence of thrombin, [Q], the molar concentration of the thrombin, k_q, the quenching rate constant, τ°, the luminescence lifetime in the absence of quencher (4.3 μs) and τ, the luminescence lifetime in the presence of quencher (1.9 μs) respectively. The quenching constant is typically obtained from the slope of a linear fit to a plot of I_0/I versus [thrombin]. However, deviations from the linear relationship are traditionally observed in certain situations outlined here: (i) when the quenching efficiency is very high, as observed in super quenching of conjugated polyelectrolytes by gold nanoparticles [58], (ii) if two fluorophore populations are present and one class is not available to the quencher [59], or (iii) if the fluorophore is being quenched both by collisions (dynamic quenching) and by complex formation with the same quencher (static quenching) [58, 60]. The nonlinear Stern-Volmer plot (Fig. S6, in supporting information) and high quenching constant value, k_q, $3.2\times10^{13}\,dm^3\,mol^{-1}\,s^{-1}$ indicate that there is a combined contribution of dynamic quenching and static quenching in the luminescence intensity of Ru(II) complex doped SiNPs-aptamer conjugate in the presence of thrombin. In this case, the Stern-Volmer plot exhibits an upward curvature, concave toward the *y*-axis at

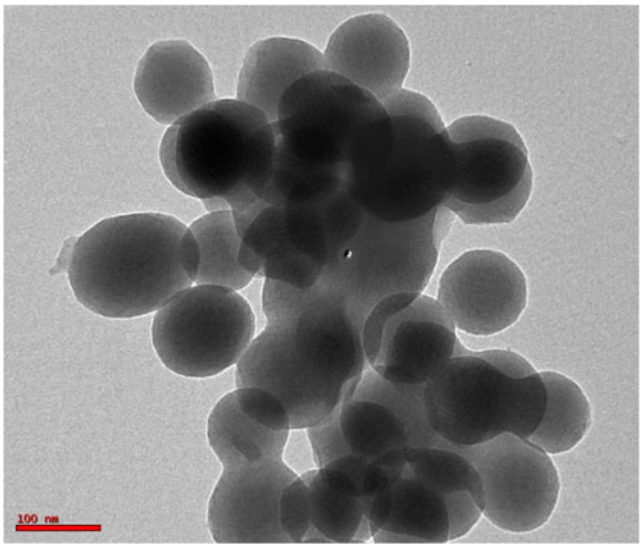

Fig. 2 TEM image of $[Ru(dpsphen)_3]^{4-}$ ion doped SiNPs-aptamer conjugates

high [Q], and Io/I is related to [Q] by the following form of the Stern-Volmer equation [58].

$$I_0/I = 1 + (K_D + K_S)[Q] + K_D K_S [Q]^2 \quad (3)$$

$$I_0/I = 1 + K_{app}[Q] \quad (4)$$

where K_D and K_S are the dynamic and static quenching constants, respectively. If there is a deviation from linearity, at high [Q] being appreciable, it is certain that both ground-state complex formation and excited-state interactions

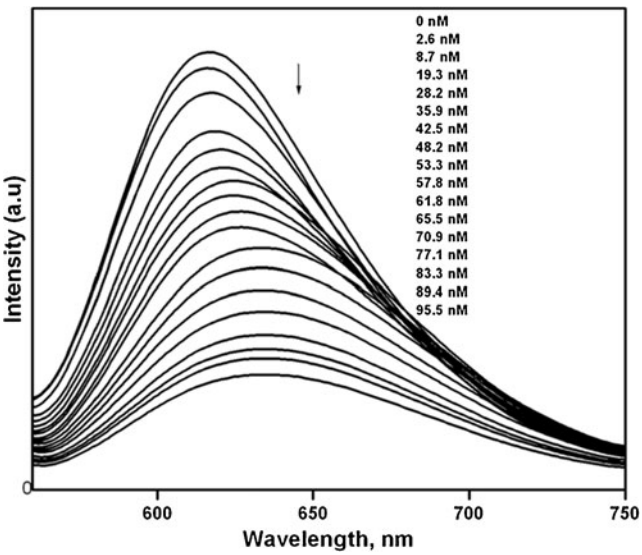

Fig. 3 Luminescence spectra of $[Ru(dpsphen)_3]^{4-}$ ion doped SiNPs-aptamer conjugates in the PBS buffer solution in the presence of different concentration of thrombin. Each spectrum was recorded with an excitation wavelength of 460 nm. The concentration of aptamer and thrombin are 100×10^{-12}M and 0–95.5×10^{-9}M respectively

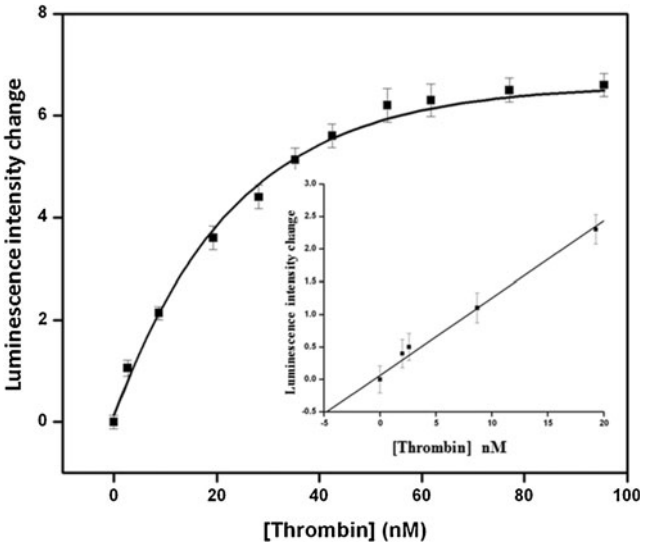

Fig. 4 Luminescence signal change of $[Ru(dpsphen)_3]^{4-}$ ion doped SiNPs-aptamer conjugate as a function of the concentration of thrombin in the PBS buffer solution. The concentration of thrombin is 0–95.5×10^{-9}M. Inset: calibration plot of thrombin sensor (R=0.983)

contribute to the quenching, which accounts for the upward curvature observed at high [Q] when both static and dynamic quenching occur for the same fluorophore. The apparent quenching constant (K_{app}) is calculated at each quencher concentration. A plot of K_{app} versus [Q] yields a straight line with an intercept of K_D+K_S and a slope of $K_S K_D$. The static and dynamic quenching constants can be obtained from the solutions of the quadratic equation. Figure S6 (in supporting information) shows the Stern-Volmer plots of I_o/I versus thrombin concentration, having substantial upward curvature, deviating from linearity. The upward curvature on quenching of luminescence intensity of Ru(II) complex doped SiNPs-aptamer conjugate in the presence of thrombin confirms a contribution of static quenching to the dynamic quenching of the fluorophore by thrombin. The upward-curving Stern-Volmer plots could be analyzed in terms of both static and dynamic quenching constants as shown in Eq. 3. The calculated dynamic (K_D) and static (K_S) static quenching constants are $2.1\times10^7 M^{-1}$ and $1.1\times10^6 M^{-1}$ respectively.

The change of emission intensity can be ascribed to the amount of thrombin bound to the sensing interface and the detection limit (4 nM) was calculated from the calibration plot. The calibration plot obtained from the straight line of the dynamic range and the detection limit was determined by 3σ/slope (σ - standard deviation of the blank measurements) [61]. The obtained detection limit was found to be lower (Table 1) than the reported aptamer assays [62–64].

Mechanism of Luminescence Quenching

We propose that the energy transfer is the major process responsible for luminescence quenching. According to

Table 1 Comparism of the thrombin sensor with other sensors

Methods	Linear range (M)	LOD(M)	Reference
Luminescence	$2.6–20\times10^{-9}$	4.0×10^{-9}	This work
Fluorescence	$10–70\times10^{-9}$	7.7×10^{-9}	[62]
Fluorescence	$10–40\times10^{-9}$	10×10^{-9}	[63]
Fluorescence	–	63×10^{-9}	[64]

Förster non-radiative energy transfer theory the rate of energy transfer depends on the extent of overlap of emission spectrum of the donor with the absorption spectrum of the acceptor and the distance between the donor and the acceptor. In addition, the energy transfer will be favorable under the following condition: i) the donor can produce florescent light that has sufficiently long lifetime; ii) the emission spectrum of the donor and the absorption spectrum of the acceptor have sufficient overlap; iii) the distance between the donor and the acceptor is less than 8 nm [65].

According to Förster's theory [65], quenching or FRET efficiency, E is given by,

$$E = \frac{R_0^6}{R_0^6 + R^6}$$

where, R_0 is the Förster radius, the distance at which transfer efficiency is 67 %, and R is the distance between the centers of the fluorophore and acceptor. Förster radius is given by Eq. (6).

$$R_0 = \left(8.8 \times 10^{23} J K^2 Q_0 n^{-4}\right) 1/6\mathrm{A} \tag{6}$$

$$J = \sum F(\lambda)\varepsilon(\lambda)\lambda^4\lambda \Big/ \sum F(\lambda)\lambda \tag{7}$$

Here, K^2 is the orientation factor for a dipole–dipole interaction, J is the spectral overlap integral in M^{-1} cm^3, Q_0 is the quantum yield of donor in the absence of acceptor, and n is the refractive index of the medium between the donor and acceptor. Fig. S7 in supporting information shows the overlap of the absorption spectrum of DABCYL with emission spectrum of the $[Ru(dpsphen)_3]^{4-}$ ion doped SiNPs. From the overlapping spectrum, J can be estimated by integrating the spectra from 560 nm to 710 nm. From this calculation, the estimated overlap integral value is 1.46×10^{-13} cm^3 mol/L and the R_0 is 4.5 nm. For this calculation we have used $K^2=2/3$ for random orientation, and $n=1.33$.

Interaction between thrombin and aptamer-SiNPs conjugate is associated with the existence of specific binding site on thrombin. Thrombin, on the surface, has two secondary binding sites. These binding sites are important for the specific interaction of thrombin with several macromolecular substrates and receptors. Of the two binding sites, one is anion-binding exosite that contributes to the formation of a tight specific complex with various substrates. The second binding site, the putative heparin recognition site, may contribute to the significant increase of thrombin inactivation by antithrombin in the presence of heparin [66, 67]. The thrombin binding aptamer has the capability to form G-quadruplex structure to recognize the fibrinogen binding exosite of thrombin via T-loop [68]. To validate the conformational change of aptamer in the presence of thrombin, we recorded the CD spectra of thrombin binding aptamer in the presence and absence of thrombin. The formation of G-quadruplex is easily characterized through the CD spectrum of positive band around 295 nm and the negative band around 270 nm respectively. The CD spectrum of thrombin binding aptamer at room temperature exhibited a negative band centered around 268 nm, and positive band around 248 nm and 290 nm in the absence of thrombin and the spectrum is shown as curve (a) in Fig. 5a. Upon the addition of thrombin to the SiNPs-aptamer conjugate a dramatic change was observed in the CD spectrum. The dramatic change of CD intensities around 268 nm and 290 nm with the addition of thrombin indicated the formation of G-quadruplex. Figure 5b shows the characteristic CD spectra of thrombin (curve a) in the absence of aptamer and in the presence of aptamer-SiNPs conjugate (curve b). Addition of aptamer leads to substantial positive shift at 215 nm and 280 nm. This result is in accordance with the previous reports [69], which show similar changes in the CD spectrum of aptamer. These results suggest that the G-quadruplex structure of thrombin binding aptamer is induced by specific interaction between aptamer and thrombin leading to substantial shift in the CD spectrum.

The surface structure and morphology of the biosensor fabrication progress is examined by AFM as shown in Fig. 6. The formation of thrombin-SiNPs-aptamer complex with the addition of thrombin to SiNPs-aptamer is confirmed using AFM technique. The AFM image of aptamer labeled SiNPs without target protein, the surface morphology, is shown in Fig. 6a. Figure 6b shows the clustered surface morphology due to the binding of thrombin to the surface of aptamer labeled SiNPs to form SiNPs-aptamer-protein complex structures. From the AFM images we learn clearly that upon the addition of the target molecule the aptamer undergoes rearrangement to form the G-quadruplex [70].

Selectivity of the Sensor System

In order to examine the selectivity of this sensor system towards thrombin, luminescence intensity measurements were carried out using various biomolucules. Thrombin is an extracellular protein that regulates many biological functions. We tested the ability of aptamers as sensor towards some common extracellular proteins, such as BSA, lysozyme, myoglobin, cytrochrome C and PDGF through the measurement of the change in emission intensity of Ru(II)

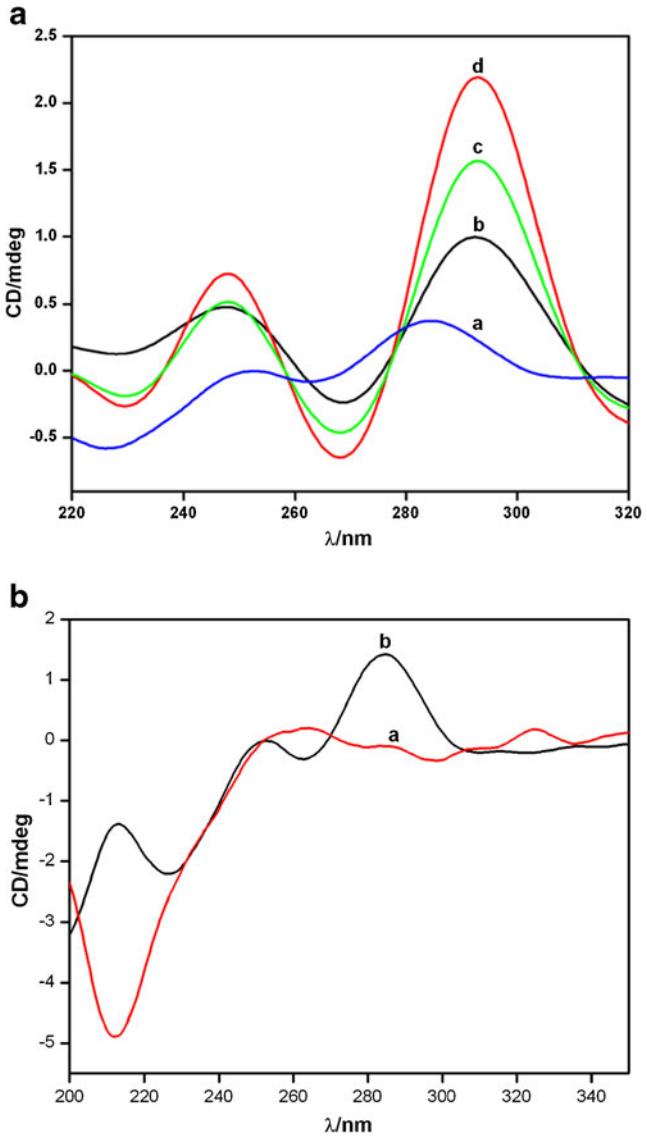

Fig. 5 **a** CD spectra of aptamer conjugated SiNPs in the absence (*curve a*) and presence (*curve b–d*) of 10, 20, 50×10^{-9}M thrombin respectively; **b** CD spectra of 0.1 μM thrombin (*curve a*) and in the presence of 100 μL of 100×10^{-12}M aptamer (*curve b*)

ion doped SiNPs-aptamer system (Fig. 7). The change in emission intensity was much higher with thrombin due to the significant interaction with aptamer. On the other hand under the similar experimental conditions there is little change in the emission intensity of luminophore doped SiNPs in the presence of other proteins. The sensitivity of the aptamer is maintained under the complex environment such as BSA and in the presence of mixture of biomolecules (Fig. S8, in supporting information). The detection limit of this sensor towards thrombin is upto 4 nM. Thus a very simple and sensitive luminescent sensor is developed for thrombin using aptamer as the receptor and Ru(II) complex doped SiNPs as the luminophore.

Label Free Detection of Thrombin

We investigated the effect of adding amine functionalized $[Ru(dpsphen)]^{4-}$ ion doped SiNPs to DABCYL labeled aptamer at room temperature (Fig. S9, in supporting information). Mixing the two solutions, amine functionalized SiNPs with the negatively charged aptamer, results in the formation of positively charged large SiNPs surrounded by smaller negatively charged aptamer [23, 71]. Luminescence quenching is observed and this is attributed to strong binding due to the electrostatic interaction between the positively charged SiNPs and the negatively charged aptamer (Fig. 8). We propose that the quenching is via energy transfer due to the close proximity of the quencher to the SiNPs surface. To investigate the efficiency of this label free system as a sensor for thrombin the emission measurements were carried out in the presence of various concentrations of thrombin. Interestingly, the addition of thrombin leads to the restoration of the emission intensity of luminescent SiNPs. Successive addition of thrombin results in successive enhancement in the emission intensity of luminescent SiNPs as shown in Fig. S10 in supporting information. From this observation we propose that the strong binding of aptamer with thrombin causes some of the aptamer molecules relieved from the SiNPs surface and a decrease in the number of aptamers on the surface of the SiNPs. Fig. S11 in supporting information shows the specificity of the aptamer towards thrombin compared with other proteins like BSA, lysozyme, myoglobin, cytrochrome C and PDGF. The binding constant (K=1.6×$10^7 M^{-1}$) was calculated using modified Benesi-Hildebrand equation shown in, Eq. (8)

$$I_0/I_0 - I = (b/a - b)(1/K[Q] + 1) \quad (8)$$

I_0 and I are the luminescence intensity of Ru(II) complex in the absence and presence of target protein, [Q] is the concentration of protein, K is the binding constant. In this equation b/a−b can be found out by plotting I_0/I_0−I versus the inverse concentration of protein, $[Protein]^{-1}$ and b/a−b, is the intercept of the Benesi-Hildebrand plot. The obtained binding constant is one order higher than the K_S value calculated from the stern-Volmer equation. The quenching sphere radius was calculated from the Perrin model [72] Eq. (9),

$$In(I_0/I) = V[Q] = (4/3\pi R_s N)[Q] \quad (9)$$

Where N-Avogadro's number, V-volume of quenching sphere and R_s is the radius of the quenching sphere. Using Eq. (9) the quenching radius of the doped SiNPs-aptamer system has been estimated to be 135 nm. It is interesting to note that when the aptamer is covalently attached to the surface of SiNPs the quenching of emission intensity of luminophore doped SiNPs occurs in the presence of thrombin. On the other hand when the luminescence measurements are carried out under the label free condition it leads to the

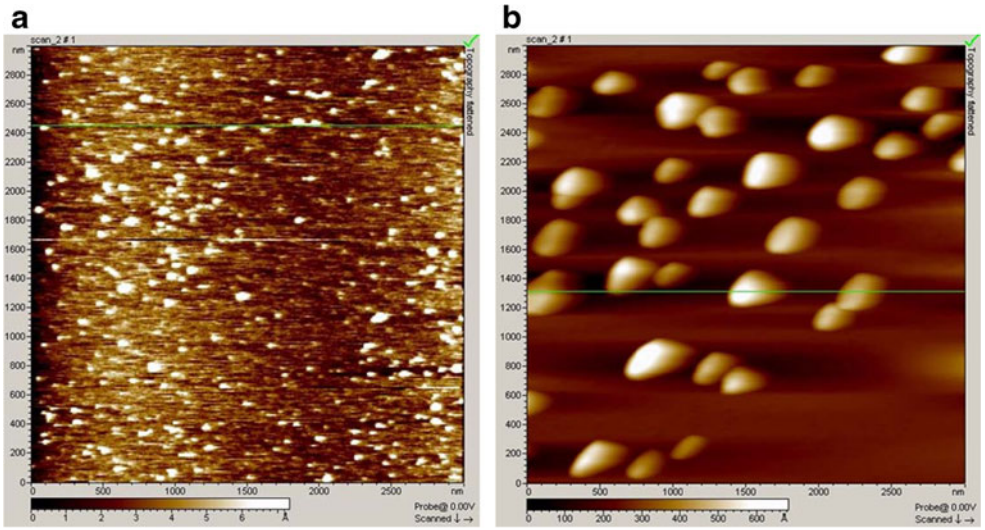

Fig. 6 AFM image of aptamer conjugated SiNPs in the absence of thrombin (**a**) and in the presence of thrombin (**b**)

luminescence enhancement. As far as we are concerned this is a novel biosensor system for the selective detection of thrombin under biological conditions using aptamers as receptors under labeled as well as label free conditions.

Conclusions

We have developed a new sensor system carrying luminescent $[Ru(dpsphen)_3]^{4-}$ ion doped SiNPs in the one end of the aptamer and the quencher DABCYL on the other end. The aptamer maintains the binding properties of the original sequence and preserves high affinity and selectivity, ensuring that the corresponding detection system possesses attractive features, low detection limit and high selectivity. The substantial change of the emission intensity observed in the presence of thrombin due to the conformational change of the aptamer i.e., from the unfolded coil conformer to folded structure of G-quadruplex is due to the energy transfer process. The exquisite sensitivity of luminescence detection is achieved using the hydrophilic $[Ru(dpshen)_3]^{4-}$ ion doped SiNPs and an aptamer in the complex environment and the detection of thrombin is at ~4 nM level. It is interesting to note that label free system rather than quenching is also an effective sensor system but substantial luminescence enhancement is observed in the presence of thrombin in the label free system. This has advantages over other strategies it is reusable by simple centrifugation. Our results indicate that the aptamer-SiNPs conjugated system is very sensitive and highly specific as sensor for thrombin, in a mixture of proteins.

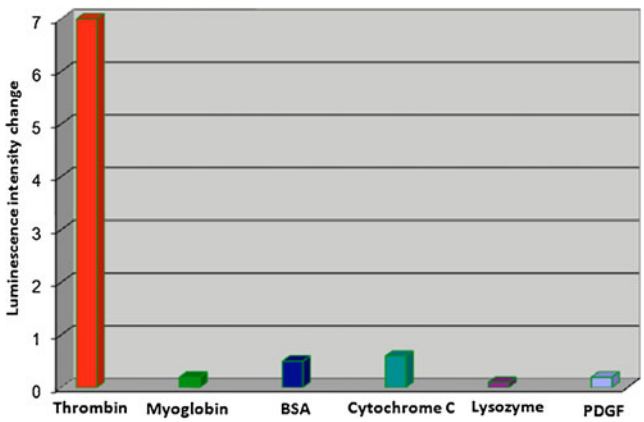

Fig. 7 Selectivity plotted in a histogram form using dye doped SiNPs-aptamer conjugated system towards thrombin. The concentration of proteins: thrombin 2.6×10^{-9}M, myoglobin 2×10^{-8}M, BSA 2×10^{-8} M, cytochrome 2×10^{-8}M, lysozyme 2×10^{-8}M, PDGF 2×10^{-8}M

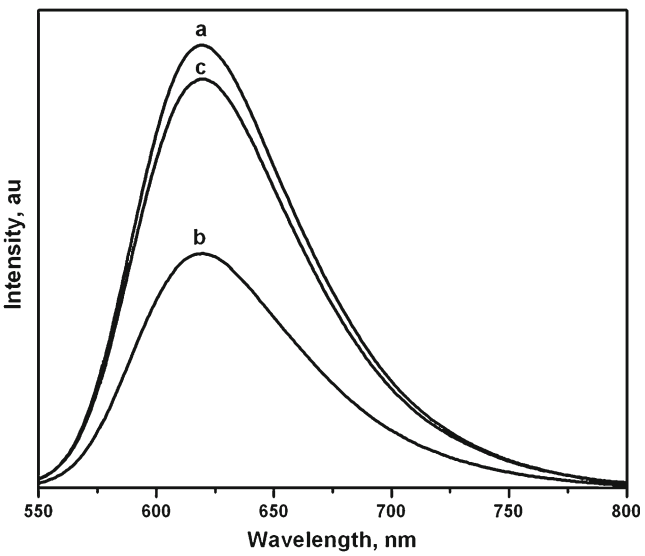

Fig. 8 Luminescence spectra of $[Ru(dpsphen)_3]^{4-}$ ion doped SiNPs before (**a**) and after addition of DNA aptamer (**b**), in the presence of thrombin (**c**) respectively

Acknowledgments This work was supported by Department of Science and Technology, New Delhi, India. We thank Prof. S. Krishnasamy and P. Manojkumar, School of Biotechnology, Madurai Kamaraj University for valuable discussions.

References

1. Ellington AD, Szostak JW (1990) In vitro selection of RNA molecules that bind specific ligands. Nature 346:818–822
2. Tuerk C, Gold L (1990) Systematic evolution of ligands by exponential enrichment: RNA ligands to bacteriophage T4 DNA polymerase. Science 249:505–510
3. Wang Y, Li J, Wang H, Jin J, Liu J, Wang K, Tan W, Yang R (2010) Silver ions-mediated conformational switch: facile design of structure-controllable nucleic acid probes. Anal Chem 82:6607–6612
4. Zhen SJ, Chen LQ, Xiao SJ, Li YF, Hu PP, Zhan L, Peng L, Song EQ, Huang CZ (2010) Carbon nanotubes as a low background signal platform for a molecular aptamer beacon on the basis of long-range resonance energy transfer. Anal Chem 82:8432–8437
5. Zhang X, Li Y, Su H, Zhang S (2010) Highly sensitive and selective detection of Hg^{2+} using mismatched DNA and a molecular light switch complex in aqueous solution. Biosens Bioelectron 25:1338–1343
6. Choi MS, Yoon M, Baeg J-O, Kim J (2009) Label-free dual assay of DNA sequences and potassium ions using an aptamer probe and a molecular light switch complex. Chem Commun 7419–7421
7. Heyduk E, Heyduk T (2005) Nucleic acid-based fluorescence sensors for detecting proteins. Anal Chem 77:1147–1156
8. Drabovich AP, Okhonin V, Berezovski M, Krylov SN (2007) Smart aptamers facilitate multi-probe affinity analysis of proteins with ultra-wide dynamic range of measured concentrations. J Am Chem Soc 129:7260–7261
9. He J-L, Wu Z-S, Zhang S-B, Shen G-L, Yu R-Q (2009) Novel fluorescence enhancement IgE assay using a DNA aptamer. Analyst 134:1003–1007
10. Chen X, Estevez M-C, Zhu Z, Huang Y-F, Chen Y, Wang L, Tan W (2009) Using aptamer-conjugated fluorescence resonance energy transfer nanoparticles for multiplexed cancer cell monitoring. Anal Chem 81:7009–7014
11. Freeman R, Sharon E, Tel-Vered R, Willner I (2009) Supramolecular cocaine-aptamer complexes activate biocatalytic cascades. J Am Chem Soc 131:5028–5029
12. Kang H, O'Donoghue MB, Liu H, Tan W (2010) A liposome-based nanostructure for aptamer directed delivery. Chem Commun 46:249–251
13. Zheng D, Seferos DS, Giljohann DA, Patel PC, Mirkin CA (2009) Aptamer nano-flares for molecular detection in living cells. Nano Lett 9:3258–3261
14. Shieh Y-A, Yang S-J, Wei M-F, Shieh M-J (2010) Aptamer-Based Tumor-Targeted Drug Delivery for Photodynamic Therapy. ACS Nano 4:1433–1442
15. Kim D, Jeong YY, Jon S (2010) A drug-loaded aptamer-gold nanoparticle bioconjugate for combined ct imaging and therapy of prostate cancer. ACS Nano 4:3689–3696
16. Zhang S, Xia J, Li X (2008) Electrochemical biosensor for detection of adenosine based on structure-switching aptamer and amplification with reporter probe DNA modified Au-nanoparticles. Anal Chem 80:8382–8388
17. Xu W, Lu Y (2010) Label-free fluorescent aptamer sensor based on regulation of malachite green fluorescence. Anal Chem 82:574–578
18. Yao W, Wang L, Wang H, Zhang X, Li L (2009) An aptamer-based electrochemiluminescent biosensor for ATP detection. Biosens Bioelectron 24:3269–3274
19. Wang J, Zhou HS (2008) Aptamer-based Au nanoparticles-enhanced surface plasmon resonance detection of small molecules. Anal Chem 80:7174–7178
20. Chhabra R, Sharma J, Ke Y, Liu Y, Rinker S, Lindsay S, Yan H (2007) Spatially addressable multiprotein nanoarrays templated by aptamer-tagged DNA nanoarchitectures. J Am Chem Soc 129:10304–10305
21. Yao C, Qi Y, Zhao Y, Xiang Y, Chen Q, Fu W (2009) Aptamer-based piezoelectric quartz crystal microbalance biosensor array for the quantification of IgE. Biosens Bioelectron 24:2499–2503
22. Attia MS, Othman AM, Aboaly MM, Abdel-Mottaleb MSA (2010) Novel spectrofluorimetric method for measuring the activity of the enzyme α-l-fucosidase using the nano composite optical sensor samarium(III)-doxycycline complex doped in sol–gel matrix. Anal Chem 82:6230–6236
23. Shenhar R, Rotello VM (2003) Nanoparticles: scaffolds and building blocks. Acc Chem Res 36:549–561
24. Mulder WJM, Strijkers GJ, Van Tilborg GAF, Cormode DP, Fayad ZA, Nicolay K (2009) Nanoparticulate assemblies of amphiphiles and diagnostically active materials for multimodality imaging. Acc Chem Res 42:904–914
25. Senarath-Yapa MD, Phimphivong S, Coym JW, Wirth MJ, Aspinwall CA, Scott Saavedra S (2007) Preparation and characterization of Poly (lipid)-coated, fluorophore-doped silica nanoparticles for biolabeling and cellular imaging. Langmuir 23:12624–12633
26. Liu D, He X, Wang K, He C, Shi H, Jian L (2010) Biocompatible silica nanoparticles-insulin conjugates for mesenchymal stem cell adipogenic differentiation. Bioconjugate Chem 21:1673–1684
27. Burns AA, Vider J, Ow H, Herz E, Penate-Medina O, Baumgart M, Larson SM, Wiesner U, Bradbury M (2009) Fluorescent silica nanoparticles with efficient urinary excretion for nanomedicine. Nano Lett 9:442–448
28. Moulari B, Pertuit D, Pellequer Y, Lamprecht A (2008) The targeting of surface modified silica nanoparticles to inflamed tissue in experimental colitis. Biomaterials 29:4554–4560
29. Qhobosheane M, Santra S, Zhang P, Tan W (2001) Biochemically functionalized silica nanoparticles. Analyst 126:1274–1278
30. Wu YF, Chen CL, Liu SQ (2009) Enzyme-functionalized silica nanoparticles as sensitive labels in biosensing. Anal Chem 81:1600–1607
31. Wang H, Yang R, Yang L, Tan W (2009) Nucleic acid conjugated nanomaterials for enhanced molecular recognition. ACS Nano 3:2451–2460
32. Arduini M, Mancin F, Tecilla P, Tonellato U (2007) Self-organized fluorescent nanosensors for ratiometric pb^{2+} detection. Langmuir 23:8632–8636
33. Wang S, Wang H, Jiao J, Chen K-J, Owens GE, Kamei K-I, Sun J, Sherman DJ, Behrenbruch CP, Wu H, Tseng H-R (2009) Three-dimensional nanostructured substrates toward efficient capture of circulating tumor cells. Angew Chem 121:9132–9135
34. Wang L, Yang C, Tan W (2005) Dual-luminophore-doped silica nanoparticles for multiplexed signaling. Nano Lett 5:37–43
35. Wang L, Zhao W, O'Donoghue MB, Tan W (2007) Fluorescent nanoparticles for multiplexed bacteria monitoring. Bioconjugate Chem 18:297–301
36. Wu H, Huo Q, Varnum S, Wang J, Liu G, Nie Z, Liu J, Lin Y (2008) Dye-doped silica nanoparticle labels/protein microarray for detection of protein biomarkers. Analyst 133:1550–1555
37. Yan J, Estevez MC, Smith JE, Wang K, He X, Wang L, Tan W (2007) Dye-doped nanoparticles for bioanalysis. Nano Today 2:44–50
38. Herr JK, Smith JE, Medley CD, Shangguan D, Tan W (2006) Aptamer-conjugated nanoparticles for selective collection and detection of cancer cells. Anal Chem 78:2918–2924
39. Wang Y, Liu B (2009) Conjugated polyelectrolyte-sensitized fluorescent detection of thrombin in blood serum using aptamer-

immobilized silica nanoparticles as the platform. Langmuir 25:12787–12793
40. Hedges SJ, Dehoney SB, Hooper JS, Amanzadeh J, Busti AJ (2007) Evidence-based treatment recommendations for uremic bleeding. Nat Clin Pract Nephrol 3:138–153
41. Nishino A, Suzuki M, Ohtani H, Motohashi O, Umezawa K, Nagura H, Yoshimoto TJ (1993) Thrombin may contribute to the pathophysiology of central nervous system injury. Neurotrauma 10:167–179
42. Serruys PW, Vranckx P, Allikmets K (2006) Clinical development of bivalirudin (Angiox®): rationale for thrombin-specific anticoagulation in percutaneous coronary intervention and acute coronary syndromes. Int J Clin Pract 60:344–350
43. Arai T, Miklossy J, Klegeris A, Guo JP, McGeer PLJ (2006) Thrombin and prothrombin are expressed by neurons and glial cells and accumulate in neurofibrillary tangles in Alzheimer disease brain. Neuropathol Exp Neurol 65:19–25
44. Vaughan PJ, Pike CJ, Cotman CW, Cunningham DD (1995) Thrombin receptor activation protects neurons and astrocytes from cell death produced by environmental insults. J Neurosci 15:5389–5401
45. Striggow F, Riek M, Breder J, Henrich-Noack P, Reymann KG, Reiser G (2000) The protease thrombin is an endogenous mediator of hippocampal neuroprotection against ischemia at low concentrations but causes degeneration at high concentrations. Proc Natl Acad Sci USA 97:2264–2269
46. Bock LC, Griffin LC, Latham JA, Vermaas EH, Toole JJ (1992) Selection of single-stranded DNA molecules that bind and inhibit human thrombin. Nature 355:564–566
47. Vairamani M, Gross ML (2003) G-quadruplex formation of thrombin-binding aptamer detected by electrospray ionization mass spectrometry. J Am Chem Soc 125:42–43
48. Zanarini S, Ciana LD, Marcaccio M, Marzocchi E, Paolucci F, Prodi L (2008) Electrochemistry and electrochemiluminescence of [Ru(II)-tris(bathophenanthroline-disulfonate)]$^{4-}$ in aprotic conditions and aqueous buffers. J Phys Chem B 112:10188–10193
49. Santra S, Zhang P, Wang K, Tapec R, Tan W (2001) Conjugation of biomolecules with luminophore-doped silica nanoparticles for photostable biomarkers. Anal Chem 73:4988–4993
50. Freeman R, Li Y, Tel-Vered R, Sharon E, Elbaz J, Willner I (2009) Self-assembly of supramolecular aptamer structures for optical or electrochemical sensing. Analyst 134:653–656
51. Jares-Erijman EA, Jovin TM (2003) FRET imaging. Nat Biotechnol 21:1387–1395
52. Wang L, Yang C, Tan W (2005) Dual-luminophore-doped silica nanoparticles for multiplexed signaling. Nano Latt 5:37–43
53. Zhang D, Wu Z, Xu J, Liang J, Li J, Yang W (2010) Tuning the emission properties of $Ru(phen)_3^{2+}$ doped silica nanoparticles by changing the addition time of the dye during the stober process. Langmuir 26:6657–6662
54. Amoroso AJ, Coogan MP, Dunne JE, Fernandez-Moreira V, Hess JB, Hayes AJ, Lloyd D, Millet C, Pope SJA, Williams C (2007) Rhenium *fac* tricarbonyl bisimine complexes: biologically useful fluorochromes for cell imaging applications. Chem Commun 3066–3068
55. Wang Y, Liu B (2007) Silica nanoparticle assisted DNA assays for optical signal amplification of conjugated polymer based fluorescent sensors. Chem Commun 3553–3555
56. Chang H, Tang L, Wang Y, Jiang J, Li J (2010) Graphene fluorescence resonance energy transfer aptasensor for the thrombin detection. Anal Chem 82:2341–2346
57. Grynyov RS, Sorokin AV, Guralchuk GY, Yefimova SL, Borovoy IA, Malyukin YV (2008) Squaraine dye as an exciton trap for cyanine j-aggregates in a solution. J Phys Chem C 112:20458–20462
58. Lakowizc JR (2006) Principles in fluorescence spectroscopy, 3rd edn. Springer, New York
59. Wu C, Peng H, Jiang Y, McNeill J (2006) Energy transfer mediated fluorescence from blended conjugated polymer nanoparticles. J Phys Chem B 110:14148–14154
60. Wu C, Szymanski C, McNeill J (2006) Preparation and encapsulation of highly fluorescent conjugated polymer nanoparticles. Langmuir 22:2956–2960
61. Zhang S, Yan Y, Bi S (2009) Design of molecular beacons as signaling probes for adenosine triphosphate detection in cancer cells based on chemiluminescence resonance energy transfer. Anal Chem 81:8695–8701
62. Huanga DW, Niua CG, Qina PZ, Ruana M, Zenga GM (2001) Time-resolved fluorescence aptamer-based sandwich assay for thrombin detection. Talanta 83:185–189
63. Hamaguchi N, Ellington A, Stanton M (2001) Aptamer beacons for the direct detection of proteins. Anal Biochem 294:126–131
64. Edwards KA, Baeumner AJ (2010) Aptamer sandwich assays: label-free and fluorescence investigations of heterogeneous binding events. Anal Bioanal Chem 398:2635–2644
65. Forster T, Sinanoglu O (eds) (1996) Modern quantum chemistry, Vol. 3. Academic, New York, p 93
66. Vu TKH, Wheaton VI, Hune DT, Charo I, Couehlin SR (1991) Domains specifying thrombin-receptor interaction. Nature 353:674–677
67. Corral-Rodrguez MA, Macedo-Ribeiro S, Pereira PJB, Fuentes-Prior P (2010) Leech-derived thrombin inhibitors: from structures to mechanisms to clinical applications. J Med Chem 53:3847–3861
68. Padmanabhan K, Tulinsky A (1996) An ambiguous structure of a DNA 15-mer thrombin complex. Acta Crystallogr D52:272–282
69. Jin Y, Bai J, Li H (2010) Label-free protein recognition using aptamer-based fluorescence assay. Analyst 135:1731–1735
70. Rinker S, Ke Y, Liu Y, Chhabra R, Yan H (2008) Self-assembled DNA nanostructures for distance-dependent multivalent ligand-protein binding. Nat Nanotechnol 3:418–422
71. Rosenholm JM, Sahlgren C, Linden M (2010) Towards multifunctional, targeted drug delivery systems using mesoporous silica nanoparticles - opportunities & challenges. Nanoscale 2:1870–1883
72. Latterini L, Amelia M (2009) Sensing proteins with luminescent silica nanoparticles. Langmuir 25:4767–4773